ACADÉMIE
DES SCIENCES
INSTITUT DE FRANCE

Comptes Rendus

Géoscience

Sciences de la Planète

Kelly Pasquon, Julien Gargani, Manish Patel, Matthew Sylvest,
Matthew Balme, Susan J. Conway, Marion Masse and Gwenael Jouannic

Experimental simulation of high mobility processes and exotic pseudolevitation

Volume 357 (2025), p. 411-423

Online since: 2 October 2025

https://doi.org/10.5802/crgeos.313

The Comptes Rendus. Géoscience — Sciences de la Planète *are a member of the Mersenne Center for open scientific publishing*
www.centre-mersenne.org — e-ISSN : 1778-7025

ACADÉMIE DES SCIENCES
INSTITUT DE FRANCE

Comptes Rendus. Géoscience — Sciences de la Planète
2025, Vol. 357, p. 411-423
https://doi.org/10.5802/crgeos.313

Research article
Geomorphology

Experimental simulation of high mobility processes and exotic pseudolevitation

Kelly Pasquon [a,b], Julien Gargani [*,a,c], Manish Patel [d], Matthew Sylvest [d], Matthew Balme [d], Susan J. Conway [e], Marion Masse [e] and Gwenael Jouannic [b]

[a] Université Paris-Saclay, Geops, CNRS, Orsay, France

[b] Cerema, Nantes, France

[c] Université Paris-Saclay, Centre d'Alembert, France

[d] Open University, Milton Keynes, UK

[e] Nantes Université, Université d'Angers, Le Mans Université, CNRS UMR 6112, Laboratoire de Planetologie et Geosciences, France

E-mails: kellypasquon@hotmail.com (K. Pasquon), julien.gargani@universite-paris-saclay.fr (J. Gargani), manish.patel@open.ac.uk (M. Patel), matthew.sylvest@gmail.com (M. Sylvest), matt.balme@open.ac.uk (M. Balme), susan.conway@univ-nantes.fr (S. J. Conway), marion.masse@univ-nantes.fr (M. Masse), gwenael.jouannic@cerema.fr (G. Jouannic)

Abstract. Planetary surfaces are transformed by various processes at different atmospheric pressures. On Mars, fluids are expected to have flowed at reduced atmospheric pressure during the last 3 billion years. Nevertheless, the influence of low pressure on surface processes has been investigated in only a few studies. Our understanding of the influence of gas in fluids on Martian surface morphologies is poor due to the low number of experiments performed at low atmospheric pressure (~7 mbar) and the limited potential analogs on Earth. Here, we present laboratory and numerical experiments to explore the influence of gas production on fluid-sand mobility at low atmospheric pressure. Energetic cohesive sand pellets uplifted by escaping gas were generated, forming narrow channels with levees with lengths of 80–90 cm, which were approximately 1800 times their widths. The maximum experimentally determined velocity of the pellets ranged from 60 to 150 cm/s. The channel morphologies were formed by a pseudo-levitation mechanism corresponding to transport with reduced friction. We propose that the mechanisms observed in our experiments at low atmospheric pressure may explain some past Martian surface changes.

Keywords. Mars, Low pressure, Friction, Mobility, Runout, Pseudolevitation, Erosion.

Funding. PNP (CNRS/CNES) and Europlanet.

Manuscript received 6 May 2024, revised 1 August 2025, accepted 10 September 2025.

1. Introduction

The physic of water-sand mixed flow is complex and the effects of low atmospheric pressure on the mixed flow dynamic are largely unexplored. Only a few studies have investigated flows under low atmospheric pressure (Jouannic, Gargani, S. Conway, et al., 2015; Massé et al., 2016; Herny et al., 2018). These experiments caused exotic morphologies. The full spectrum of morphological diversity has not yet been studied. Many parameters and conditions have not been investigated. Previous studies have focused on

*Corresponding author

flows under low atmospheric pressure: (i) caused by pure liquid water released over a sandy substrate with a low surface temperature, <278 K (Jouannic, Gargani, S. Conway, et al., 2015), (ii) caused by pure liquid water released over a sandy substrate with surface temperatures reaching values >290 K (Herny et al., 2018), (iii) caused by pure ice melting and sublimation on a substrate with a low surface temperature (Massé et al., 2016). In this study, a mixed flow (sand–water) is released over a sandy substrate with a temperature >290 K. The study of mixed flow at low atmospheric pressure is conducted for basic science purposes, but could also be used to discuss exotic processes that may have occurred on Mars.

Mars is thought to have experience of reduced atmospheric pressure for more than three billion years compared to Earth (Kite et al., 2014), below the triple point of water. The drop in atmospheric pressure has occurred during the last three billion years (ibid.) and the influence of atmospheric pressure lowering on morphologies is not well constrained. The variation in atmospheric pressure may have occurred with the variable presence of liquid water. An ocean is believed to have existed 3.5 Gyr ago (Di Achille and Hynek, 2010) and perhaps until the late Hesperian (Turbet and Forget, 2019). The presence of liquid water on Early Mars has also been suggested by various observations, such as fluvial and coastal (ocean) morphologies (Malin and Edgett, 2003; Di Achille and Hynek, 2010). Geomorphological and modeling studies have suggested that transient wet conditions may have occurred during the Hesperian (Baker et al., 1991), and radar observations have indicated that subglacial water bodies could still be present beneath the poles of Mars (Orosei et al., 2018; Lauro et al., 2021). Potentially, liquid water may have been present during the long transition from high to reduced atmospheric pressure on Mars. On Mars, low atmospheric pressure and transient liquid water may have existed simultaneously in the past, even if this combination of conditions is controversial in explaining many current processes (Thomas et al., 2010; Pilorget and Forget, 2015; Schimdt et al., 2017; Pasquon, Gargani, Massé, et al., 2019). In any case, the physics of flows under exotic conditions (i.e. 7 mbar) is not well known and the aim of this study is to describe such flows.

The propagation of liquid water and sediments interacting under low-pressure conditions representative of present-day Mars (~7 mbar) is complex (Massé et al., 2016). Under low atmospheric pressure (~7 mbar), their transition phase thresholds of water are significantly different than those at current terrestrial atmospheric pressure: liquid water boils near its freezing point, rather than 100 °C, under terrestrial conditions. Recent studies have shown that exotic processes may have occurred or are occurring on Mars, resulting in mechanisms and morphologies that differ from those on Earth (Massé et al., 2016; Raack et al., 2017; Herny et al., 2018; Sylvest et al., 2016; Brož et al., 2020). These surface transformation mechanisms at reduced atmospheric pressure are important because of the extended period of time Mars has spent in this atmospheric pressure regime. Mars is thought to have transitioned to low atmospheric pressure more than 3 Gyr ago (Kite et al., 2014). Surface transport, erosion and sedimentation processes may have been very different and caused exotic morphologies or different erosion and sedimentation rates over this period. On Earth, reduced atmospheric pressure less than half that of the present time existed 2.7 Gyrs ago (Som et al., 2012), which may have influenced erosion and deposition processes as temperatures could more easily reach water's boiling point (<80 °C at this atmospheric pressure).

Many complex morphological changes caused by fluid flow must be considered under low atmospheric pressures due to the various ways in which liquids and gases can modify the topography. Terrestrial analogs are generally used to interpret planetary flow dynamics; however, this approach is not entirely appropriate for describing low-pressure processes on Mars. Fluid-sediment interactions at low atmospheric pressures have been described in a few specific cases using experimental setups (S. J. Conway et al., 2011; Jouannic, Gargani, S. Conway, et al., 2015; Massé et al., 2016; Sylvest et al., 2016; Raack et al., 2017). However, considering the recent interest in this research topic, the high morphological variability of flows at low pressures has not been described exhaustively, and numerous phenomena and processes remain unknown. Here we investigate, using an experimental and theoretical approach, the transport processes associated with the propagation of wet sand over a sandy surface. The resulting dynamic and morphologies will be described and discussed.

2. Method

2.1. *Experimental setup*

To understand the influence of low atmospheric pressure on sediment propagation by a fluid (liquid or gas), a set of laboratory experiments was performed in an atmospheric chamber (Mars chamber at the Open University) with a controlled atmospheric pressure of 7 mbar. Experiments were conducted along a 20° inclined metallic surface 1 m in length and 40 cm in width covered by sand. A reservoir containing a cold (274 K < T < 278 K) mixture of water and sand was released over a hot (291 K < T < 294 K) thin (1–2 mm) non-cohesive dry sand layer placed on the inclined surface. The reservoir is 6 cm in width, 6 cm in height and >10 cm in length, and was located 4 cm above the surface at a slope of 50°. The sand layer on the surface was composed of grain sizes 200–250 μm. The sand in the reservoir was of constant mass (i.e., 50 g) and a variable mass of water ranging from 0 g to 100 g was added. Consequently, the ratio between the water and sand mass $m_{\text{water}}/m_{\text{sand}}$ ranged from 0 to 2. The variable mass ratio between water and sand was conducted in 17 experiments and allow us the measurement of 135 channels (length, width) formed by the propagation of the material. Even if a small discontinuity could be observed in a channel, it is considered as a unique channel in the counting. If two different paths with erosive features, diverging from a unique point, are observed, they are counted as two different channels. In this study, the movement analysis (distance, speed, and time) focused on the pellets that moved over longer distances using video analysis. Measurements were also performed manually, but also using image and video analysis to determine the width, length, and thickness of the resulting morphologies. Two cameras have been used to make photos and videos of the flows. Measurements accuracy were 0.5 mm. Video analysis was performed using the open-source software Kinovea.

2.2. *Numerically modeling transport and gas escape*

The interpretation of the transport process was also conducted using a modeling approach. Basically, during the propagation of the material (i.e. the pellet) along the path, gas escape from the transported material and interact with the substrate. The contact between the pellet and the substrate was simulated by a numerical model. The friction was described by the equation $\tau = \sigma_n \tan\phi$, where σ_n is the normal stress and ϕ is the kinetic friction angle. The normal stress σ_n was calculated by considering the normal component of the weight of the flow on the sliding surface as $\sigma_n = \rho_s g\, z \cos\theta$, where θ is the local slope, z is the thickness of the pellet, g is gravity and ρ_s is the density of the cohesive sand. The value of ϕ is usually considered to be >20° (e.g., Kleinhans et al., 2011). On Earth and Mars, the dynamic angle of repose of dry sand dunes ranges from 30° to 35° (Atwood-Stone and McEwen, 2013). We did not use a more sophisticated formulation of the kinetic friction coefficient (e.g., Jop et al., 2006) because this coefficient has less influence on the final results than the uncertainty in the parameters in the more complex descriptions.

The rheological expression was substituted into the Newton's laws of motion, taking into account the weight of the pellet ($F_G = mg$), the lift force exerted by escaping gas ($F_L = 0.5 C_{\text{D}} \rho_{\text{gas}} S\, v_{\text{gas}}^2$) and the friction force ($F_R = \sigma_n \tan\phi x S$), where m is the mass of the pellet, S is the surface at the base of the pellet, C_{D} is the drag coefficient, ρ_{gas} is the gas density, and v_{gas} is the velocity of the gas escaping from the pellet perpendicular to the slope.

The resulting motion along the path is described by:

$$m \cdot g \cdot \sin\theta - (\sigma_n^{\text{eff}} \tan\phi) x S = m\, \mathrm{d}v_x/\mathrm{d}t \qquad (1)$$

where t is the time, v_x is the velocity along the slope, and

$$\sigma_n^{\text{eff}} = (mg\cos\theta - 0.5 C_{\text{D}} \rho_{\text{gas}} S v_{\text{gas}}^2)/S \qquad (2)$$

and θ is the slope. The 1-D finite difference model for the dynamic equation of motion (1) was solved numerically along the slope using a finite difference approach leading to the equation:

$$v_x(t+\Delta t) = v_x(t) + [g \cdot \sin\theta - (\sigma_n^{\text{eff}} \tan\phi) x S/m] x \Delta t \qquad (3)$$

Alternatively, the pellet dynamics along the path can be simulated by a 1-D equation considering that

$$\sigma_n^{\text{eff}} \tan\phi = \sigma_n \mu_{\text{eff}} \qquad (4)$$

or equivalently that

$$\mu_{\text{eff}} = [\sigma_n^{\text{eff}} \tan\phi]/\sigma_n. \qquad (5)$$

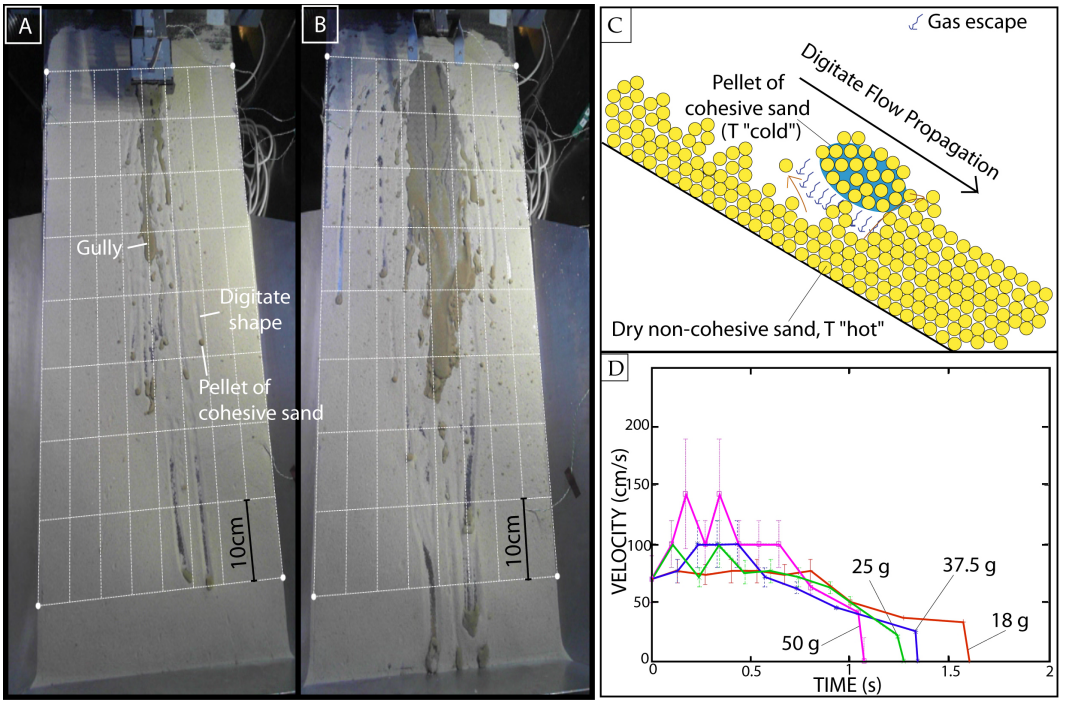

Figure 1. Morphology of linear channel, pellet and digitate flow at low atmospheric pressure for (A) a reservoir water content of 25 g and 50 g of sand and (B) a reservoir water content of 50 g and 50 g of sand. (C) Schematic representation of the pellet of wet sand during transport in our experiments. (D) Measurement of velocity versus time for different sand–water ratios (50 g of sand with 18 g, 25 g, 37.5 g or 50 g of water) using video analysis. The slope is 20°, the sand has a grain size of 200–250 μm, the cohesive wet cold sand ranges in temperature from 275 K < T < 278 K, and the hot substrate temperature ranges from 291 K < T < 294 K in all experiments. The atmospheric pressure is 7 mbar.

In this case, the reduced effective friction can be written as

$$\mu_{\text{eff}} = [1 - (0.5 C_{\text{D}} \rho_{\text{gas}} v_{\text{gas}}^2)/(gH\cos\theta\rho_{\text{sand}})]\dot{x}\tan\phi = \tan\phi_{\text{eff}} \quad (6)$$

where H is the pellet thickness. Thus, in this case, the equation that describes the motion of the pellet is

$$m \cdot g \cdot \sin\theta - \sigma_n \mu_{\text{eff}} S = m\,\mathrm{d}v_x/\mathrm{d}t \quad (7)$$

where ϕ_{eff} is the effective kinetic friction angle. In both models, the gas escape velocity v_{gas} is considered to be equal to 90 ms^{-1}, as estimated by Massé et al. (2016).

3. Results

3.1. *Experimental results*

We observed an exotic mass transport process that we call digitate flow because it produces multiple narrow channels with a linear path (Figure 1). Two other morphologies are also observed: (i) a linear channel caused by the mixing flow of sand and liquid water, with some minor signs of boiling (bubbles, sand ejection) and (ii) a low-density flow composed of "individual" sand grains that were transported tens of centimeters above the experimental surface, as a cloud of sand. However, the second process did not influence the morphology. We focus on the digitate flow morphology, which has never been accurately described before. Various digitate shapes were observed (1–25, Figures 1 and 2), including long (80–90 cm) and narrow (5–10 mm, Figure 1) channels. They were formed by the rapid propagation (60–150 cm/s) of small pellets of wet sand with a maximum diameters of ~2 ± 0.5 mm. Substrate erosion to a depth of about 1 mm, lateral levees and a frontal levee at the end of the path are the main morphological features of the channel caused by the

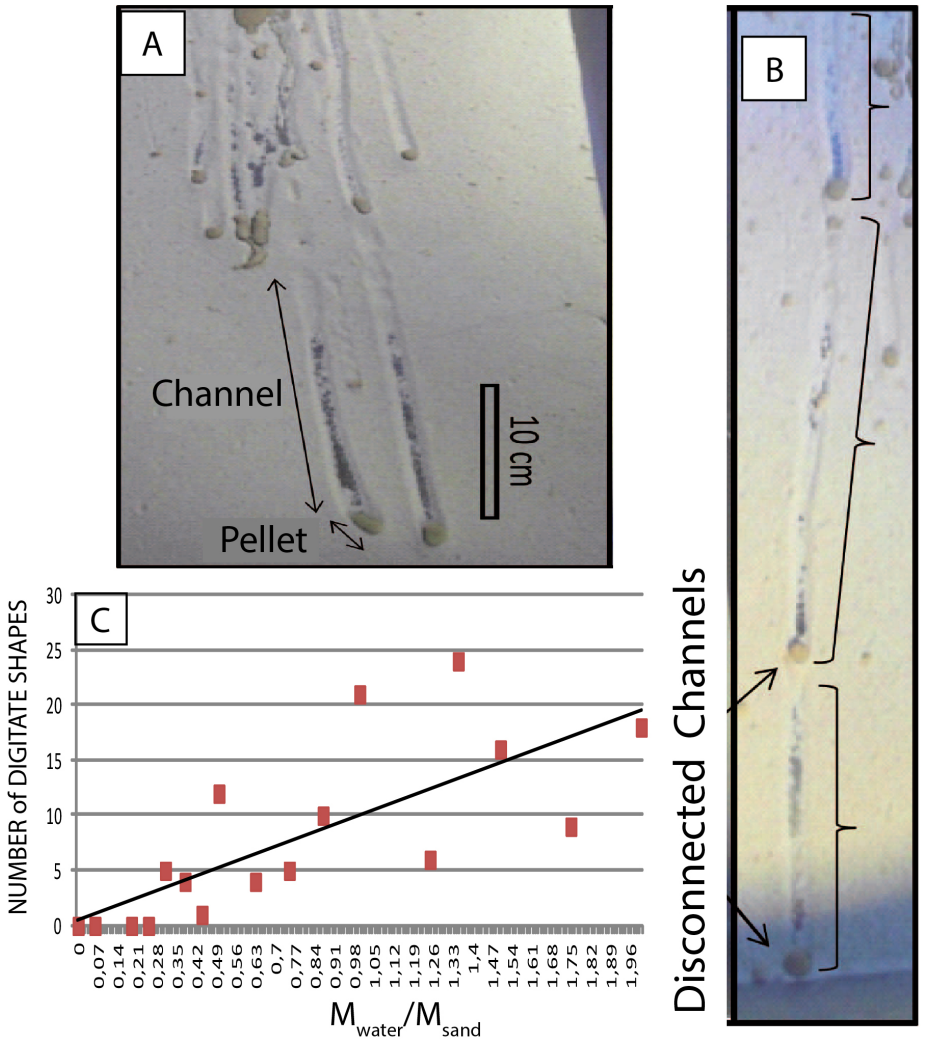

Figure 2. Experiment at low atmospheric pressure. (A) Annotated view of the channels produced by the pellets. (B) Pellet channels with gaps after splitting. (C) Influence of the sand–water ratio $M_{\text{water}}/M_{\text{sand}}$, where M is the mass, on the number of digitate shapes (i.e. pellet-channels).

pellet propagation. The pellets formed rapidly after contact with the substrate, and their size remained constant during the flow, as indicated by the constant channel width. The pellets rapidly (1.5–2 s) generated a channel-like morphology (~1 mm deep) with lateral levees ~1 mm high on the substrate due to the displacement of the sand substrate by the direct contact of the pellet and its escaping gas. No liquid flow or liquid diffusion occurs in these channels, as evidenced by the light color of the substrate (contrary to the darker color of the wetted substrate in the same experiment), which is why this process is called dry digitate flow.

As the wet sand pellet propagates, water vapor is produced at the interface between the cold pellet (274 K < T < 278 K) and the hot sand substrate (291 K < T < 294 K). The energetic gas escape from the pellet causes sand grains to be ejected from the substrate to the outside of the channel. These channels can have one or two gaps along their path due to some short (~1 cm) rebound/levitation events that may be sometimes associated with the

pellet splitting. The maximum velocity of the pellets is not influenced by the initial amount of sand in our experiments. The dry digitate flows are always produced during less than 2 s in all experiments. The velocity of the pellets gradually increases along their path, reaching a maximum velocity of approximately 60–150 cm/s, before decelerating rapidly. However, the number of channels produced by the pellet (i.e. digitate shapes) depends on the initial mass of liquid water (Figure 2). The higher the water content of the reservoir, the greater the number of digitate shapes observed. Furthermore, higher water mass in the reservoir leads to faster pellet motion (Figure 1). The release of additional water vapor during the splitting may explain why the pellets move over a longer period of time and faster. The pellets split when the water content is higher. When the pellets split, it could cause (i) two divergent channels, (ii) one or more rebounds associated with disconnection along the channel, (iii) different propagation length of the new formed pellets (Figure 2).

The results of the numerical modeling were then validated by comparison with the experimental results, and next, the pellet motion under Martian gravity and other kinds of gas escape was simulated.

3.2. *Reduced effective friction and pseudo-levitation modeling results*

Even if one or two short rebound/levitation events occur, the flow has permanent or semi-permanent contact with the substrate, as shown by the semi-continuous morphologies of the channel and lateral levees along the path. The pellet dynamics and digitate shape morphology cannot be explained by pure levitation processes ($\mu_{\text{eff}} = 0$) but can be explained by reduced effective friction $\mu_{\text{eff}} = \tan\phi_{\text{eff}}$. The gas escape from the pellet displaces some isolated dry sand grains, moving the grains away from their initial position on the substrate. However, the pellet has permanent or semi-permanent contact with the substrate, as suggested by the formation of lateral and frontal levees and erosion of the channel. The semi-permanent contact is characterized by pellet rebounds and small channel disconnections along the pellet path. The process that causes the dry digitate shapes is not a pure levitation process due to the permanent or semi-permanent contact between the pellet and the sand substrate: it will be called pseudo-levitation. We fit the experimental observations via simulations, considering a gas escape speed of v_{gas} of 90–100 ms^{-1} and a drag coefficient $C_{\text{D}} = 1.18$, as in Massé et al. (2016), at the beginning of the dry digitate flow, along ~40–70 cm of the path, i.e., from $t = 0.45$–0.8 s (Figure 3). Then, the rapid decrease in the lift force produced by the gas escape until $F_L = 0$ increases the effective friction and abruptly decreases the pellet velocity. These results were obtained considering a pellet thickness of 2 ± 0.5 mm (Figure 3A and 2B). The gas escape allows a sliding propagation over a longer distance and a higher slip propagation speed than without gas escape or with a smaller velocity of gas escape. The presence of a lift force caused by the escaping gas is equivalent to a reduced effective friction $\mu_{\text{eff}} \sim 0.2$ ($\phi_{\text{eff}} \sim 11.5°$) along the first ~40–70 cm ($t = 0.45$–0.8 s) of the path before the friction increases to the friction of the dry sand, i.e., $\mu_{\text{eff}} = \mu = 0.58$ ($\phi \sim 30°$, Figure 3A).

3.3. *Modeling the high mobility process under Martian conditions*

The numerical simulations suggest that under Martian gravitational conditions ($g_{\text{Mars}} = 3.72$ ms^{-2}), the mobility of the sediments could be multiplied by more than 3 for pellet propagation (Figure 3B). For a pellet of 1.5 mm thickness and a gas escape of 0.45 s, our model suggests that the path length reaches ~290 cm under Martian gravitational conditions instead of the ~90 cm path length observed under terrestrial gravitation conditions. For a 2.5 mm thick pellet and a gas escape of 0.8 s, our model suggests that the path length reaches ~360 cm under Martian gravity instead of the ~90 cm path length observed under Earth gravity (Figure 3C). Moreover, when the Martian gas density of $(CO_2)_{\text{gas}}$ is considered instead of $(H_2O)_{\text{gas}}$, the simulated mobility increases by more than 4 times (Figure 4C).

4. Discussion

4.1. *Comparison with previous experimental results*

From a physical point of view, the experimentally obtained velocity (i.e., 60–150 cm/s) is greater than the erosion threshold of sand (Gargani, 2004).

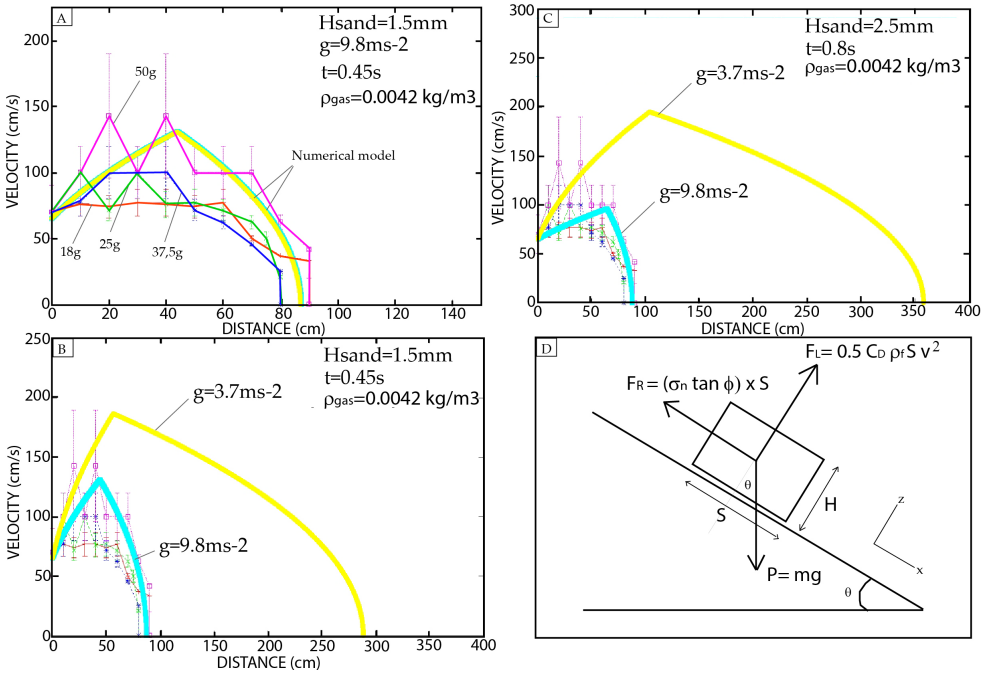

Figure 3. Dynamics of pellet propagation. (A) Experimental and numerical model velocity vs. distance, with $C_D = 1.18$, a gas escape speed v_{gas} of 90 ms^{-1} at $t = 0.45$ s, a simulated pellet thickness of 1.5 mm, and an initial velocity of 70 cm/s. $\phi = 30°$ in the blue simulation, and $\phi_{eff} = 11.5°$ in the yellow simulation. (B) Influence of gravity on the pellet velocity and runout. The blue simulation parameters are identical to those used in the previous graph, i.e., $C_D = 1.18$, the gas speed v_{gas} is 90 ms^{-1} at $t = 0.45$ s, $\phi = 30°$, and the initial velocity is 70 cm/s. In the yellow simulation, $g = 3.72$ ms^{-2}. (C) Pellet velocity and runout simulation for a pellet thickness of $H = 2.5$ mm, $C_D = 1.18$ and a gas speed v_{gas} of 90 ms^{-1} at $t = 0.8$ s, $\phi = 30°$, and an initial velocity of 70 cm/s. (D) Force diagram. In all the experiments, as in the numerical models, the slope θ is 20°.

The experimentally obtained velocity is also faster than the propagation velocity observed in flows in previous low-pressure experiments for gullies obtained with a release of a pure water flow over a frozen surface (Jouannic, Gargani, S. Conway, et al., 2015) or a "hot" surface until 297 K (Herny et al., 2018), and for the melting of a water ice block over a thin dry sand surface (Massé et al., 2016). The experimental speed obtained in this study is also slightly faster than the propagation of pellet described in Herny et al. (2018) of 75 cm/s at the maximum.

4.2. *Possible Martian landforms analogs*

4.2.1. *Past Martian conditions and potential analogs*

During the last billions of years, low atmospheric pressure (Kite et al., 2014), diurnal temperatures >290 K, and a higher availability of liquid water than during the late Amazonian are believed to have existed on Mars. Consequently, pseudo-levitation processes could have been common in the past on Mars. The degradation of old Martian surfaces could cause difficulties in identifying the morphologies formed by these processes. During the last million/billion years, numerous processes may have degraded the present surface of Mars and explain the lack of accurate observations: Aeolian processes (Balme and Greeley, 2005), degradation by sublimation processes (Séjourné, Costard, Gargani, Soare, Fedorov, et al., 2011; Séjourné, Costard, Gargani, Soare and Marmo, 2012), crater impacts (Lagain et al., 2021).

4.2.2. *Debris flows and seasonal activities on Mars*

Debris flow morphologies on Mars suggest the presence of high mobility processes due to the

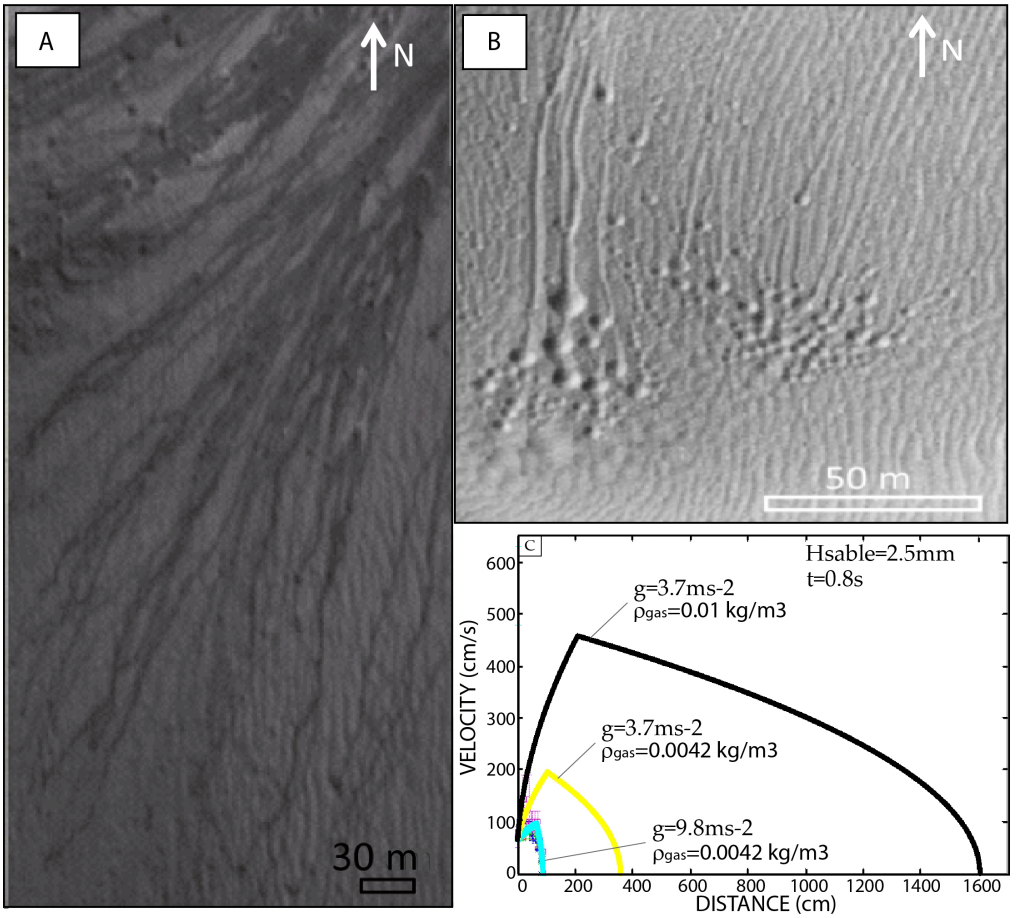

Figure 4. (A) Morphologies on the Kaiser dune in the HiRISE image ESP_018608_1330, Mars, described in Pasquon, Gargani, Nachon, et al. (2018). (B) Linear dune gullies and pits on the Matara dune, Mars, HiRISE image ESP_038,255_1300. (C) Velocity and runout simulation for CO_2 (ρ_{gas} = 0.01 kg/m^3 in Diniega et al., 2013) and H_2O (ρ_{gas} = 0.0042 kg/m^3) gas flux. Here, C_D = 1.18, the gas escape speed is 90 ms^{-1} at t = 0.8 s, ϕ = 30°, and the initial velocity is 70 cm/s. In all the numerical models, the slope θ is 20°.

presence of ice, evaporite, gas or liquid water (De Blasio, 2011; Lucas et al., 2014). The occurrence of past and present high mobility processes on Mars are compatibles with the potential role of processes uncommon on Earth caused under different pressure-temperature conditions. On Mars, high mobility processes are inferred by morphologies observed on gentle slopes of 6–8°, such as the linear gullies of the Russell megadune (Jouannic, Gargani, Costard, et al., 2012) or the perennial rill (Jouannic, S. J. Conway, et al., 2018). Linear gullies are around 1 km in length, with a 10 m width and lateral levees height of 1 m (Pasquon, Gargani, Massé and S. Conway, 2016). Perennial rills are morphologies with a width of 1 m that growth seasonally during springtime a few hundreds of meters along sand dunes, with an increasing number of channels from upstream to downstream (Jouannic, S. J. Conway, et al., 2018). The high mobility of sand for hundreds of meters along gentle slopes could be due to the presence of CO_2 (Pasquon, Gargani, Massé, et al., 2019) and H_2O on and below the surface (Jouannic, Gargani, Costard, et al., 2012; Jouannic, S. J. Conway, et al., 2018) or brines (Chevrier, 2025). On Mars, CO_2 ice

is seasonally present on the surface and is known to influence seasonal surface changes (Pilorget and Forget, 2015; Pasquon, Gargani, Massé, et al., 2019). The controversial presence of hydrated salt on the surface after recurring slope lineae (RSL) formation has been interpreted as a potential proof of the existence of a transient liquid water phase (Ojha et al., 2015), but a dry granular flow is an alternative interpretation (Schimdt et al., 2017). Deep groundwater has been proposed as the origin of this water (Abotalib and Heggy, 2019). The experimental morphologies obtained in this study (lateral levees, eroded channel) are different from the ones of the RSL and do not appear to be a potential analog. Thick water ice deposits can also be observed (Dundas et al., 2018), which may influence the transport processes for granular material and the evolution of surface morphology. The aim of this study is not to argue for or against the presence of liquid water or brines on Mars at the present time, but only to test the role of gas ejection from a solid pellet on the propagation process on a slope and on morphologies.

4.2.3. *Martian gullies*

The experimental morphologies are characterized by a channel with a linear morphology (length ≫ width), lateral levees, a final pit at the end of the intermediate channels and several aligned disconnected channels. From a morphological point of view, some unexplained Martian morphologies present similar characteristics, such as long, linear, narrow, partially disconnected channels with lateral levees and aligned pits diverging from gullies (Figures 2 and 4; Pasquon, Gargani, Nachon, et al., 2018). In the experiments, the pellet is deposited at the end of the last channel, whereas Martian morphologies do not always show a final deposit (Pasquon, Gargani, Massé and S. Conway, 2016; Diniega et al., 2013). On Mars, the final pit feature has been explained by the sublimation of icy blocks (Diniega et al., 2013).

The morphology of the degraded water-rich or ice-rich deposits is different from the morphology of fresh deposits (Jouannic, Gargani, S. Conway, et al., 2015), and this could cause difficulties or misinterpretation of these morphologies. The degradation of pellets could occur in a few hours or days. The resulting morphologies are difficult to observe when pellets become dry and the sand becomes noncohesive. The resulting morphology could be very small. An ice-rich block to reach pluri-meter scale is certainly easier to be observed than a wet sand pellet of 1 m without ice, due to the cohesive properties of ice. For morphologies with width equal or superior to 1 m, initial cohesion of the pellet must be considered: ice-rich blocks or pure ice are better explanatory material than wet sand. The repetition of ice-rich blocks sliding along the same path could increase the channel width and length. Seasonal water frost thickness on Mars could reach 1 mm (mean thickness 180 μm; Lange et al., 2024) and seasonal CO_2 frost/snow thickness could reach 2 m at high latitude (Smith et al., 2001). The sublimation rate of ice (CO_2 and H_2O ice) could reach values ranging from 0.74 mm/h for water ice (Chittenden et al., 2008) to 80 cm/s for CO_2 ice (Cedillo-Flores et al., 2011). However, in specific conditions, water ice sublimation is believed to reach 0.3 m/s (Kim et al., 2022) and CO_2 ice 5–15 m/s (Thomas et al., 2010). A gas escape of 80 cm/s is sufficient to cause pseudo-levitation of centimeter-thick blocks.

The experimentally obtained velocity is less than the modeling estimations based on Manning's equation applied to gullies morphologies along the Russell megadune on Mars (Mangold et al., 2010; Jouannic, Gargani, Costard, et al., 2012). Our model suggests that a velocity similar to those of Jouannic, Gargani, Costard, et al. (2012) and Mangold et al. (2010) could be reached on a gentle slope of 7–8° by assuming a low effective friction coefficient of 0.2 (i.e., ϕ_{eff} = 11°–11.5°, Figure 5). Theoretically, this low effective friction coefficient could be obtained from pseudo-levitation of sand mixed with liquid water, but it is not excluded that sand mixed with water ice, or with CO_2 ice, may generate sufficient sublimation (i.e. gas escape from ice) to cause similar transport processes and morphologies. Pseudo-levitation of ice–rich material containing CO_2 ice could be produced by a minimum gas speed of 80 cm/s for fluidization of CO_2 gas under Martian conditions (Cedillo-Flores et al., 2011).

4.3. *Implications for terrestrial flows*

4.3.1. *Early earth*

On Earth, lower atmospheric pressure is thought to have occurred 2.7 Gyrs ago (Som et al., 2012), which may have influenced surface processes. However, weathering conditions and plate tectonics

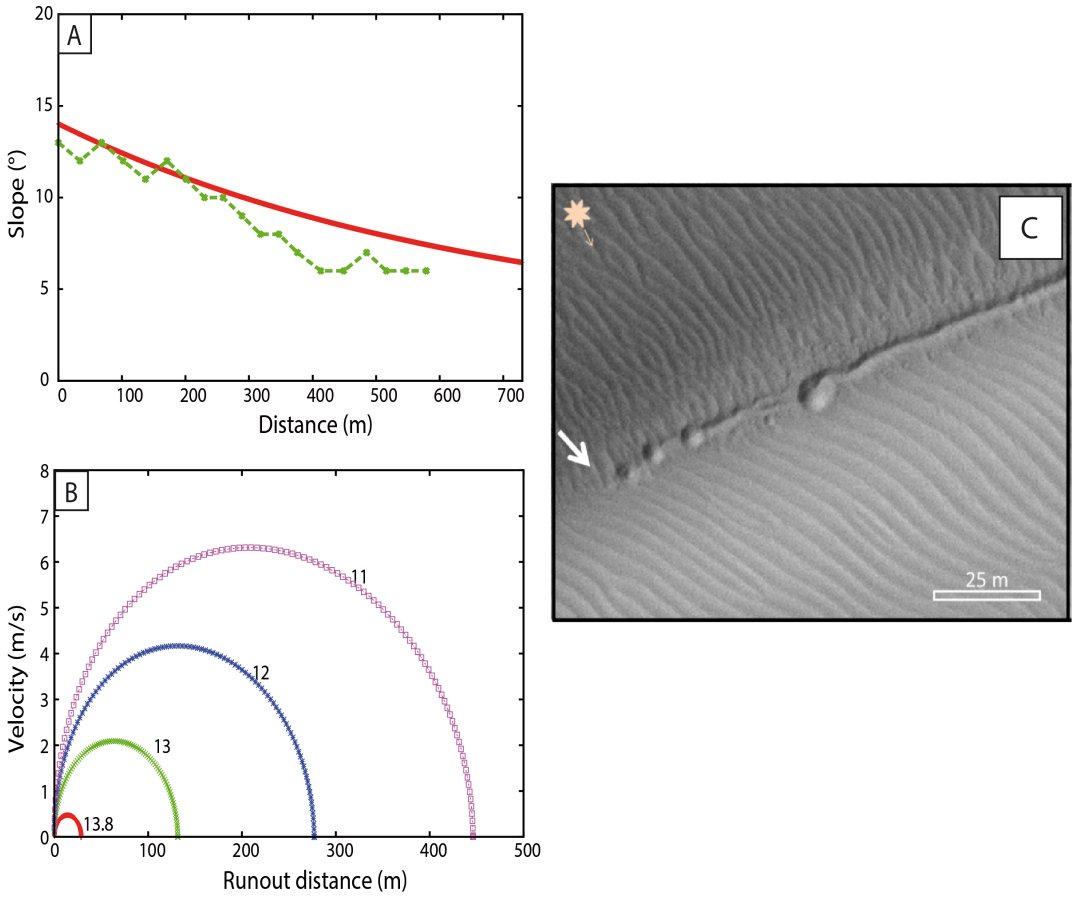

Figure 5. Numerical modeling of sand displacement along a slope. (A) The slope θ as a function of the distance x in the area where the perennial rills are located. The green curve is the slope extracted from the HRSC DTM, and the red curve is the smooth decrease in the slope, which is used as an input in the numerical simulation. (B) Velocity of the simulated granular flows as a function of the runout distance for various kinetic effective friction angles ϕ_{eff}, including $\phi_{\text{eff}} = 11°$, 12°, 13° and 13.8°, assuming that the initial velocity is zero. Due to noise in the HRSC DTM and for simplicity, the topography is smoothed by assuming that the height follows $H(x) = H_0 \exp(-x/L_0)$, where x is the distance along the sliding path and H_0 and L_0 are two empirical constants. In the model, $H_0 = 100$ m, $L_0 = 400$ m and $g_{\text{Mars}} = 3.72$ ms^{-2}. (C) Linear dune gullies with disconnected pits on Matara dune, Mars described in Pasquon, Gargani, Nachon, et al. (2018), HiRISE image ESP_020,770_1300.

caused the destruction or non-preservation of old and rare morphologies in the rock record. The experiments conducted in this study allow us to discuss the potential role of boiling water on the mobility of terrestrial surface processes. When the atmospheric pressure is half the present atmospheric pressure (Som et al., 2012), the boiling point occurs for lower temperatures (<80 °C) and could be more frequent.

4.3.2. *Pyroclastic flows analog*

Several experimental studies investigated the role of fluidization in granular flows to understand pyroclastic flows (Roche, Gilbertson, et al., 2004; Roche, Buesch, et al., 2016). Our experimental flows reached maximum speeds of 1–1.5 ms^{-1}, which is in the range of experimental studies of pyroclastic flows released by fluidized granular columns with high interstitial

air pore pressure at ambient temperature and pressure (Roche, Buesch, et al., 2016). In our experiments, the Froude number Fr = $v_{\text{pellet}}/(g^{\cdot} H_{\text{pellet}})^{1/2}$ ranged between 3 and 4, which is slightly larger than the value of 2.4–2.8 observed in pyroclastic flows (Roche, Gilbertson, et al., 2004).

There are too many differences between our experiments and pyroclastic flow to pretend that it is a perfect analog. However, the influence of gas escape on mobility in both cases is relevant to discuss the role of gas escape. Pyroclastic flows are characterized by high mobility (Valentine and Wohletz, 1989; Gueugneau et al., 2017) and significant velocity (Calder et al., 1999). During pyroclastic flows, the rock degassing process or gas escape in the dense current causes increased mobility. The runout of granular flow is increased by fluidization (Roche, Gilbertson, et al., 2004). Gas is expected to decrease the friction basal shear stress, which affects the motion of solid materials. Effective normal stress reduction justifies the use of low effective friction coefficients for pyroclastic density currents (Breard et al., 2018). The morphology of pyroclastic flows includes central channels, lateral levees and abrupt termination. In Montserrat, the friction of pyroclastic flows has been evaluated to range from 0.3 to 0.06 based on morphological observations of the length and height, whereas cold-debris avalanches display a wider range of friction values ranging from 0.5 to 0.03 (Calder et al., 1999). During pyroclastic flows, speeds of 3–25 ms^{-1} have been observed (Cole et al., 1998; Calder et al., 1999; Yamamoto et al., 1993; Roche, Buesch, et al., 2016).

Explosively ejected hot ballistics or hot pyroclastic debris on snow slopes could also cause water vapor and snow melting and trigger volcanic ice-slurry flows, volcanic mixed avalanches and lahars. Volcanic ice-slurry flows and mixed avalanches are characterized by low friction processes and occur during natural events that involve mixing hot volcanic material, ice, snow, water and air (Kataoka et al., 2021; Pierson and Janda, 1994). The melting of glacier ice and snow by pyroclastic density currents or phreatic explosions is a common process causing liquefied and lubricated flows (Lube et al., 2009). Gas is not necessarily present along the entire path but may play a role during the beginning of this phenomenon when hot volcanic rocks (Cronin et al., 1996) and/or explosive events (Waythomas et al., 2013) are involved. High mobility (i.e., 0.13–0.16), a significant velocity of 5–14 ms^{-1} and frontal Froude numbers >6 have been estimated for volcanic ice-slurry flows (Lube et al., 2009). The presence of gas in the initial phase during this kind of event suggests potential applications of our experiments and models, to pyroclastic flows.

4.4. *Ice-rich slope on Galilean satellites of Jupiter?*

During the last decades, the presence of various icy and water-rich environments has been described in the solar system. More specifically, three of the four icy moons of Jupiter (Europe, Ganymede, Callisto) are known to be ice-rich, but also to have a liquid water ocean in depth, in the case of Europe and Ganymede (Spohn and Schubert, 2003). In the case of Europe, some geysers of liquid water have been observed (Reynolds et al., 1983; Steinbrügge et al., 2020). Surface processes associated with the presence of water ice and liquid water under low atmospheric pressure on these moons are still unknown. Future mission JUICE may help to describe more accurately the surface evolution of these extreme environments (Grasset et al., 2013) and allow us to discuss transport mobility on their surfaces.

5. Conclusion

We performed several material transport experiments at a low atmospheric pressure of 7 mbar along a 20° slope. These experiments allowed us to observe exotic transport processes involving multiple (1–25) divergent pellets of wet sand. These generated erosive channels with lateral and frontal levees. Gas escaped from the cold pellets that contacted the hot substrate via boiling. The velocity of this exotic transport process reached 60 to 150 cm/s over distances of 80–90 cm. This high mobility process is caused by the pseudo-levitation of the wet sand pellets. This exotic transport can be formalized by a reduced effective friction coefficient. A dry digital flow produced by the reduced effective friction in relation to CO_2 or H_2O gas escaping at the interface between a water-rich cold sand pellet and a relatively hot substrate is a possible mechanism that may have transformed the surface of Mars. This kind of process can influence planetary surfaces and may have caused surface erosion in prior Martian history.

Acknowledgments

This study was funded by the PNP (CNRS/CNES) and Europlanet. The editorial board, and especially François Chabaux, is acknowledged for their work.

Declaration of interests

The authors do not work for, advise, own shares in, or receive funds from any organization that could benefit from this article, and have declared no affiliations other than their research organizations.

References

Abotalib, A. Z. and E. Heggy, "A deep groundwater origin for recurring slope lineae on Mars", *Nat. Geosci.* **12** (2019), pp. 235–241.

Atwood-Stone, C. and A. S. McEwen, "Avalanche Slope angles in low-gravity environments from active Martian sand dunes", *Geophys. Res. Lett.* **40** (2013), pp. 2929–2934.

Baker, V. R., R. G. Strom, V. C. Gulick, J. S. Kargel, G. Komatsu and V. S. Kale, "Ancient oceans, ice sheets and the hydrological cycle on Mars", *Nature* **352** (1991), pp. 589–594.

Balme, M. and R. Greeley, "Dust devils on Earth and on Mars", *Rev. Geophys.* **44** (2005), article no. RG3003.

Breard, E. C. P., J. Dufek and G. Lube, "Enhanced mobility in concentrated pyroclastic density currents: an examination of a self-fluidization mechanism", *Geophys. Res. Lett.* **45** (2018), pp. 654–664.

Brož, P., O. Krýza, L. Wilson, et al., "Experimental evidence for lava-like mud flows under Martian surface conditions", *Nat. Geosci.* **13** (2020), no. 6, pp. 403–407.

Calder, E. S., P. D. Cole, W. B. Dade, et al., "Mobility of pyroclastic flows and surges at the Soufriere Hills Volcano, Montserrat", *Geophys. Res. Lett.* **26** (1999), no. 5, pp. 537–549.

Cedillo-Flores, Y., A. H. Treiman, J. Lasue and S. M. Clifford, "CO_2 gas fuidization in the initiation and formation of Martian plar gullies", *Geophys. Res. Lett.* **38** (2011), article no. L21202.

Chevrier, V. F., "Perchlorate brine formation from frost at the Viking 2 landing site", *Commun. Earth Environ.* **6** (2025), article no. 447.

Chittenden, J. D., V. Chevrier, L. A. Roe, K. Bryson, R. Pilgrim and D. W. G. Sears, "Experimental study effect of wind on the stability of water ice on Mars", *Icarus* **196** (2008), pp. 477–487.

Cole, P. D., E. S. Calder, T. H. Druitt, R. Hoblitt, R. Robertson, R. S. J. Sparks and S. R. Young, "Pyroclastic flows generated by gravitational instability of the 1996–97 lava dome of Soufriere Hills Volcano, Montserrat", *Geophys. Res. Lett.* **25** (1998), no. 18, pp. 3425–3428.

Conway, S. J., M. R. Balme, J. B. Murray, M. C. Towner, C. H. Okubo and P. M. Grindrod, "The indication of martian gully formation processes by slope–area analysis", *Geol. Soc. Lond. Spec. Pub.* **356** (2011), no. 1, pp. 171–201.

Cronin, S. J., V. E. Neall, J. A. Lecointre and A. S. Palmer, "Unusual "snow slurry" lahars from Ruapehu volcano New Zealand, September 1995", *Geology* **24** (1996), no. 12, pp. 1107–1110.

De Blasio, F. V., "Landslides in Valles Marineris (Mars): A possible role of basal lubrication by sub-surface ice", *Planet. Space Sci.* **59** (2011), no. 13, pp. 1384–1392.

Di Achille, G. and B. M. Hynek, "Ancient ocean on Mars supported by global distribution of deltas and valleys", *Nat. Geosci.* **3** (2010), pp. 459–463.

Diniega, S., C. J. Hansen, J. N. Mcelwaine, C. H. Hugenholtz, C. M. Dundas, A. S. McEwen and M. C. Bourke, "A new dry hypothesis for the formation of martian linear gullies", *Icarus* **225** (2013), pp. 526–537.

Dundas, C. M., A. M. Bramson, L. Ojha, et al., "Exposed subsurface ice sheets in the Martian mid-latitudes", *Science* **359** (2018), pp. 199–201.

Gargani, J., "Contribution à l'étude de la vitesse critique d'érosion des sols cohésifs", *C. R. Géosci.* **336** (2004), pp. 561–566.

Grasset, O., M. K. Dougherty, A. Coustenis, et al., "JUpiter ICy moons Explorer (JUICE): an ESA mission to orbit Ganymede and to characterise the Jupiter system", *Planet. Space Sci.* **78** (2013), pp. 1–21.

Gueugneau, V., K. Kelfoun, O. Roche and L. Chupin, "Effects of pore pressure in pyroclastic flows: numerical simulation and experimental validation", *Geophys. Res. Lett.* **44** (2017), pp. 2194–2202.

Herny, C., S. J. Conway, J. Raack, S. Carpy, T. Colleubanse and M. R. Patel, "Downslope sediment transport by boiling liquid water under Mars-like conditions: experiments and potential implications for Martian gullies", *Geol. Soc. Lond. Spec. Publ.* **467** (2018), pp. 373–410.

Jop, P., Y. Forterre and O. Pouliquen, "A constitutive law for dense granular flows", *Nature* **441** (2006), pp. 727–730.

Jouannic, G., S. J. Conway, J. Gargani, et al., "Morphological characterization of landforms produced by springtime seasonal activity on Russell Crater megadune, Mars", *Geol. Soc. Lond. Spec. Publ.* **467** (2018), pp. 115–144.

Jouannic, G., J. Gargani, S. Conway, et al., "Laboratory simulation of debris flows over a sand dune: insights into gully-formation (Mars)", *Geomorphology* **231** (2015), pp. 101–115.

Jouannic, G., J. Gargani, F. Costard, G. Ori, C. Marmo, F. Schmidt and A. Lucas, "Morphological and mechanical characterization of gullies in a periglacial environment: the case of the Russell crater dune (Mars)", *Planet. Space Sci.* **71** (2012), pp. 38–54.

Kataoka, K. S., K. Tsunematsu, T. Matsumoto, A. Urabe and K. Kawashima, "Crisis hazard assessment for snow-related lahars from an unforeseen new vent eruption: the 2018 eruption of Kusatsu-Shirane volcano, Japan", *Earth Planet. Space* **73** (2021), article no. 220.

Kim, Y., D. Jewitt, J. Agarwal, M. Mutchler, J. Li and H. Weaver, "Hubble space telescope observations of active asteroid P/2020 O1 (Lemmon-PANSTARRS)", *Astrophys. J. Lett.* **933** (2022), article no. L15.

Kite, S. E., J.-P. Williams, A. Lucas and O. Aharonson, "Low paleopressure of the Martian atmosphere estimated from the size distribution of ancient craters", *Nat. Geosci.* **7** (2014), pp. 335–339.

Kleinhans, M. G., H. Markies, S. J. de Vet, A. C. in't Veld and F. N. Postema, "Static and dynamic angles of repose in loose granular materials under reduced gravity", *J. Geophys. Res. Planets* **116** (2011), article no. E11004.

Lagain, A., S. Bouley, D. Baratoux, et al., "Crater database: a participative project for the classification of large martian craters morphological characteristics", in *Large Meteorite Impacts and Planetary Evolution VI* (Reimold, W. U. and C. Koeberl, eds.), Geological Society of America, 2021.

Lange, L., S. Piqueux, C. S. Edwards, F. Forget, J. Naar, E. Vos and A. Szantai, "Observations of water frost on Mars with THEMIS: application to the presence of brines and the stability of (sub)surface water ice", *J. Geophys. Res.: Planet.* **129** (2024), article no. e2024JE008489.

Lauro, S. E., E. Pettinelli and G. Caprarelli, "Multiple subglacial water bodies below the south pole of Mars unveiled by new MARSIS data", *Nat. Astron.* **5** (2021), pp. 63–70.

Lube, G., S. J. Cronin and J. N. Procter, "Explaining the extreme mobility of volcanic ice-slurry flows, Ruapehu volcano, New Zealand", *Geology* **37** (2009), pp. 15–18.

Lucas, A., A. Mangeney and J.-P. Ampuero, "Frictional velocity-weakening in landslides on Earth and on other planetary bodies", *Nat. Commun.* **5** (2014), article no. 3417.

Malin, M. C. and K. S. Edgett, "Evidence for persistant flow and aqueous sedimentation on Early Mars", *Science* **302** (2003), pp. 1931–1934.

Mangold, N., A. Mangeney, V. Migeon, V. Ansan, A. Lucas, D. Baratoux and F. Bouchut, "Sinuous gullies on Mars: frequency, distribution, and implications for flow properties", *J. Geophys. Res.* **115** (2010), article no. E11001.

Massé, M., S. J. Conway, J. Gargani, et al., "Transport processes induced by metastable boiling water under Martian surface conditions", *Nat. Geosci.* **9** (2016), pp. 425–428.

Ojha, L., M. B. Wilhelm, S. L. Murchie, A. S. McEwen, J. J. Wray, J. Hanley, M. Massé and M. Chojnacki, "Spectral evidence for hydrated salts in recurring slope lineae on Mars", *Nat. Geosci.* **8** (2015), pp. 829–832.

Orosei, R., S. E. Lauro, E. Pettinelli, et al., "Radar evidence of subglacial liquid water on Mars", *Science* **361** (2018), no. 6401, pp. 490–493.

Pasquon, K., J. Gargani, M. Massé, et al., "Present-day development of gully-channel sinuosity by carbon dioxide gas supported flows on Mars", *Icarus* **329** (2019), pp. 296–313.

Pasquon, K., J. Gargani, M. Massé and S. Conway, "Present-day formation and seasonal evolution of linear dune gullies on Mars", *Icarus* **274** (2016), pp. 195–210.

Pasquon, K., J. Gargani, M. Nachon, et al., "Are different martian gully morphologies due to different processes on the Kaiser dune field?", *Geol. Soc. Lond. Spec. Publ.* **467** (2018), pp. 145–164.

Pierson, T. and R. J. Janda, "Volcanic mixed avalanches: a distinct eruption-triggered mass-flow process at snow-clad volcanoes", *GSA Bull.* **106** (1994), no. 10, pp. 1351–1358.

Pilorget, C. and F. Forget, "Formation of gullies on Mars by debris flows triggered by CO_2 sublimation", *Nat. Geosci.* **9** (2015), no. 1, pp. 65–69.

Raack, J., S. J. Conway, C. Herny, M. R. Balme, S. Carpy and M. R. Patel, "Water induced sediment levitation enhances downslope transport on Mars", *Nat. Commun.* **8** (2017), article no. 1151.

Reynolds, R. T., S. W. Squyres, D. S. Colburn and C. P. Mckay, "On the habitability of Europa", *Icarus* **56** (1983), pp. 246–254.

Roche, O., D. C. Buesch and G. A. Valentine, "Slow-moving and far-travelled dense pyroclastic flows during the Peach Spring super-eruption", *Nat. Commun.* **7** (2016), article no. 10890.

Roche, O., M. A. Gilbertson, J. C. Philips and R. S. J. Sparks, "Experimental study of gas-fluidized granular flows with implications for pyroclastic flow emplacement", *J. Geophys. Res.* **109** (2004), article no. B10201.

Schimdt, F., F. Andrieu, F. Costard, M. Kocifaj and A. G. Meresescu, "RSL as dry granular flows induced by natural pump", in *Lunar and Planetary Science XLVIII, Houston, USA*, 2017. Online at https://repository.hou.usra.edu/server/api/core/bitstreams/8c7d6460-72df-472f-8068-aa16de7d52f3/content (accessed on July 30, 2025).

Séjourné, A., F. Costard, J. Gargani, R. Soare, A. Fedorov and C. Marmo, "Scalloped depressions and small-sized polygons in western Utopia Planitia, Mars: a new formation hypothesis", *Planet. Space Sci.* **59** (2011), pp. 412–422.

Séjourné, A., F. Costard, J. Gargani, R. Soare and C. Marmo, "Evidence of an aeolian ice-rich and stratified permafrost in Utopia Planitia, Mars", *Planet. Space Sci.* **60** (2012), pp. 248–254.

Smith, D. E., M. T. Zuber and Neumann G. A., "Seasonal variations of snow depth on Mars", *Science* **294** (2001), no. 5549, pp. 2141–2146. PMID: 11739951.

Som, S., D. Catling, J. Harnmeijer, P. Polivka and R. Buick, "Air density 2.7 billion years ago limited to less than twice present levels by fossil raindrop imprints", *Nature* **484** (2012), pp. 359–362.

Spohn, T. and G. Schubert, "Oceans in the icy Galilean satellites of Jupiter", *Icarus* **161** (2003), pp. 456–467.

Steinbrügge, G., J. R. C. Voigt, N. S. Wolfenbarger, et al., "Brine migration and impact-induced cryovolcanism on Europa", *Geophys. Res. Lett.* **47** (2020), article no. e2020GL090797.

Sylvest, M. E., S. J. Conway, M. R. Patel, J. C. Dixon and A. Barnes, "Mass wasting triggered by seasonal CO_2 sublimation under Martian atmospheric conditions: laboratory experiments", *Geophys. Res. Lett.* **43** (2016), no. 24, pp. 12363–12370.

Thomas, N., C. J. Hansen, G. Portyankina and P. S. Russell, "HiRISE observations of gas sublimation-driven activity in Mars' southern polar regions: II. Surficial deposits and their origins", *Icarus* **205** (2010), pp. 296–310.

Turbet, M. and F. Forget, "The paradoxes of the Late Hesperian Mars ocean", *Sci. Rep.* **9** (2019), article no. 5717.

Valentine, G. A. and K. H. Wohletz, "Environmental hazards of pyroclastic flows determined by numerical models", *Geology* **17** (1989), pp. 641–644.

Waythomas, F. C., T. C. Pierson, J. J. Major and W. E. Ecott, "Columinous ice-rich lahars generated during the 2009 eruption of Redoubt Volcano, Alaska", *J. Volcanol. Geotherm. Res.* **259** (2013), pp. 389–413.

Yamamoto, T., S. Takarada and S. Suto, "Pyroclastic flows from the 1991 eruption of Unzen volcano, Japan", *Bull. Volcanol.* **55** (1993), pp. 166–175.